ceramics

MDPI

Article

Characterization of $ZnWO_4$, $MgWO_4$, and $CaWO_4$ Ceramics Synthesized in the Field of a Powerful Radiation Flux

Gulnur Alpyssova [1], Viktor Lisitsyn [2], Zhanara Bakiyeva [1], Ivan Chakin [3], Ekaterina Kaneva [4], Dmitriy Afanasyev [1], Ainura Tussupbekova [1,*], Vitalii Vaganov [5], Aida T. Tulegenova [6] and Serik Tuleuov [1]

[1] Department of Radiophysics and Electronics, Faculty of Physics and Technology, Karaganda University named after E.A. Buketov, Karaganda 100024, Kazakhstan; gulnur-0909@mail.ru (G.A.); shanar83@mail.ru (Z.B.); a_d_afanasyev@mail.ru (D.A.); serik.tu123@gmail.com (S.T.)
[2] Department of Lasers and Lighting Engineering, National Research Tomsk Polytechnic University, Tomsk 634050, Russia; lisitsyn@tpu.ru
[3] Budker Institute of Nuclear Physics Russian Academy of Sciences, Novosibirsk 630090, Russia; chak_in2003@bk.ru
[4] X-ray Analysis Laboratory, Vinogradov Institute of Geochemistry SB RAS, Irkutsk 664033, Russia; kev604@mail.ru
[5] Department of Materials Science, National Research Tomsk Polytechnic University, Tomsk 634050, Russia; nba_vitas@mail.ru
[6] National Nanotechnology Laboratory, Al-Farabi Kazakh National University, Almaty 050040, Kazakhstan; tulegenova.aida@gmail.com
* Correspondence: tussupbekova.ak@gmail.com; Tel.: +7-77-8219-1022

Abstract: This paper presents the results of a study on the morphology, structure, and luminescent properties of ceramics synthesized in the radiation field of $MeWO_4$ compositions (where Me is Mg, Ca, and Zn). The synthesis of ceramics was carried out by the direct action of the electron flux on an initial mixture of powders of the given stoichiometric composition. WO_3, ZnO, MgO, and CaO powders with particle sizes in the range of 1–50 microns were used for the synthesis of the samples. It was found that the yield of the radiation synthesis reaction (the ratio of the mass of the sample and the charge used), when treated with an electron flux with an energy of 1.4 MeV and a flux power density of 15–18 kW/cm^2, was in the range of 75–99%. The synthesis of all compositions was carried out under the same radiation treatment modes, although the melting temperatures of the starting materials varied significantly and ranged from 1473 °C (WO_3) to 2825 °C (MgO). The study of the ceramic structure showed that under the radiation effect of powerful radiation fluxes on the charge, a crystalline phase of the appropriate composition formed, regardless of the synthesis modes. The results of XRD studies show that during the radiation treatment of the charge, ceramics are formed mainly with the crystalline phases $ZnWO_4$, $MgWO_4$, and $CaWO_4$. These resulting $MeWO_4$ ceramics can be used for the same purposes as crystals. Photoluminescence (PL) and cathodoluminescence (CL) were studied under excitation using stationary ultraviolet radiation and nanosecond pulses of electron flux. In general, the PL and CL of synthesized ceramic samples $ZnWO_4$, $MgWO_4$, and $CaWO_4$ showed that their luminescent properties are similar to those of luminescence in corresponding crystalline materials. This indicates the formation of a crystalline phase in synthesized ceramic samples.

Keywords: ceramic; metal tungstate; radiation synthesis; electron flux; cathodoluminescence; photoluminescence

Citation: Alpyssova, G.; Lisitsyn, V.; Bakiyeva, Z.; Chakin, I.; Kaneva, E.; Afanasyev, D.; Tussupbekova, A.; Vaganov, V.; Tulegenova, A.T.; Tuleuov, S. Characterization of $ZnWO_4$, $MgWO_4$, and $CaWO_4$ Ceramics Synthesized in the Field of a Powerful Radiation Flux. *Ceramics* **2024**, *7*, 1085–1099. https://doi.org/10.3390/ceramics7030071

Academic Editor: Frank Kern

Received: 23 July 2024
Revised: 15 August 2024
Accepted: 16 August 2024
Published: 19 August 2024

1. Introduction

Tungstates of transition metals with the general formula $MeWO_4$, where Me refers to alkali–earth metals (Ca, Mg) [1–3] and transition group metals such as Pb, Cd, Zn, Co, Ni [4–6] are one of the main materials used as scintillation materials [7–10]. Metal tungstates are characterized by high material densities and luminescence bands in the

visible wavelength range from approximately 400 to 500 nm [2,3,11–13]. These materials are not hygroscopic. In terms of light output, metal tungstates are inferior to alkali-galloid crystals, but they are more resistant to radiation exposure. The tungstates of metals as wide-band semiconductors are promising for use as sensors to determine humidity [14], photocatalysts [15], and biomedical applications [16]. A number of recently published papers have shown the prospects of using lead tungsten and zinc tungstate as scintillation detectors [17,18].

The most common methods for the synthesis of metal tungstates are the methods of Chokhralsky [19,20] and Bridgman [21], which allow the synthesis of optically transparent crystals. However, carrying out synthesis using such methods is time-consuming, energy-consuming, and requires a long time to realize. Other methods of synthesizing tungstate metal crystals and ceramics are also being developed. Some types of these methods include the hydrothermal method [21], the sol-gel method [22], and other methods [6,22]. One of the most promising methods for the synthesis of ceramics from dielectric and wide-band semiconductor materials is the method of radiation synthesis [23,24]. Radiation synthesis is an express method and has several advantages. This method allows the synthesis of ceramics from precursors (charge) with very different melting temperatures. The formation of ceramics by the radiation method is realized in second range (~1–10 s), only from the charged materials and at the expense of radiation energy. The possibility of the radiation synthesis of ceramics based on $MeWO_4$ was shown by the authors in [23]. This work is devoted to the study of the morphology, structure, and luminescent properties of ceramics synthesized in the radiation field of $MeWO_4$ compositions (where Me is Mg, Ca, and Zn).

2. Materials

2.1. Morphology of Samples

The synthesis of ceramics was realized by the direct action of the electron flux on an initial mixture of powders of a given composition. The necessary electron flows were provided by electron accelerators developed and manufactured at the G.I. Budker Institute of Nuclear Physics of the Siberian Branch of the Russian Academy of Sciences (INP SB RAS). The accelerators generate electron fluxes from 0.5 to 3 MeV with a beam power of up to 100 kW. The UNU Stand ELV-6 installation, based on an accelerator generating an electron beam with energies in the range from 1.4 to 2.5 MeV and a power of up to 100 kW, was used for the synthesis. The electron beam was discharged into the open atmosphere through a differential pumping system and had a Gaussian distribution in the cross-section. In our experiments, the derived beam had a diameter of 1 cm on the target. A scanning system was used for obtaining samples of a large area. The electron beam scanned a sample with a frequency of 50 Hz over the surface of the mixture in the transverse direction of a 5 cm wide crucible. The crucible shifted relative to the scanning beam at a speed of 1 cm/s along the entire length of the crucible. In order to identify the possible dependence of the synthesis results on the modes of action of the electron beam on the charge, the synthesis mode "no scan" was used. In the "no scan" synthesis mode, the crucible was stretched relative to the stationary electron beam. During synthesis in this mode, the power density of the electron flux was reduced by four times to obtain an equivalent dose of absorbed energy [23]. The total exposure time of the electron flux to the treated surface of the charge in the crucible was always 10 s. The result of the synthesis was to obtain samples in the form of plates with a crucible size of 10×5 cm^2 or several samples with the appearance of frozen droplets. The synthesis of ceramics was realized only at the expense of the energy of the radiation flux and only from the charge materials, without the addition of other materials to facilitate the process.

WO_3, ZnO, MgO, and CaO powders from Hebei Suoyi New Material Technology Co., Ltd., and powders obtained from Chemreactive salons with a purity of at least 99.95% were used for the synthesis of the $ZnWO_4$, $MgWO_4$, and $CaWO_4$ ceramic samples. The starting materials had significantly different melting points: WO_3 (1473 °C), ZnO (1975 °C), CaO (2572 °C), and MgO (2825 °C). The efficiency of radiation synthesis depends heavily on the

particle sizes of the powders, as shown in [25]. The dispersion of the initial powders used for synthesis was studied by laser diffraction using the Shimadzu SALD-7101 laser particle size analyzer. All the raw powders used had a wide range of particle sizes. In all powders, the number of small particles with sizes from 10 to 200 nm was much greater than the larger ones with sizes of 0.2–50 microns. However, the volumes of larger micro-sized particles significantly exceeded the volumes of nanoscale particles. The synthesis efficiency was determined as the ratio of the mass of synthesized samples to the mass of the charge. The efficiency was in the range of 75–99%. Therefore, the result of synthesis was determined mainly by the volume of large particles. According to the synthesis, the results showing the measurements of the distribution of particles by their volume and by their number are shown in Figure 1.

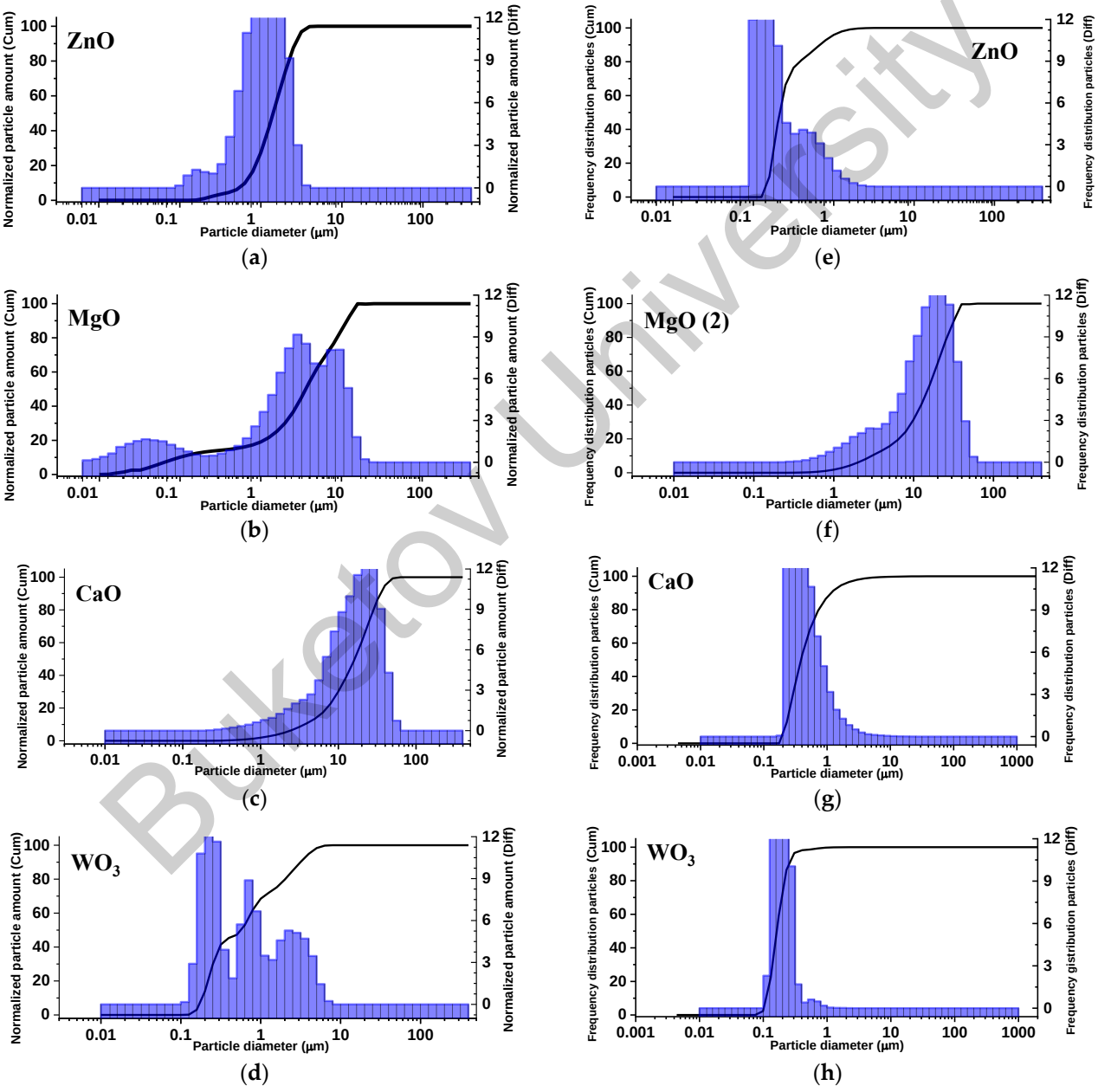

Figure 1. Particle size distribution of metal oxide powder particles based on their volume (**a**) ZnO (**b**) MgO (**c**) CaO, and (**d**) WO_3 and their number (**e**) ZnO (**f**) MgO (**g**) CaO, and (**h**) WO_3.

It can be seen that the initial powders of metal oxides used for synthesis had different particle size distributions by volume and number (See Figure 1). This difference in

dispersion did not affect the result of the synthesis using the thermal method. Due to the difference in the ratio of particle sizes of different compositions, the rate of element exchange between the particles of the starting materials in a solid- or liquid-phase medium may decrease during thermal synthesis. It can always simply increase the time of the synthesis or annealing time. The rate of exchange of elements was determined by the lifetime of the intermediate products during the radiation synthesis. The exchange of elements was carried out mainly in the local areas of the charge. Therefore, for the radiation synthesis, not only the general stoichiometry of the powder mixture was important, but also local stoichiometry. The local stoichiometry was observed when the size of particles of different compositions in the mixture was equal or close [25].

For the synthesis of $MeWO_4$ ceramic samples (where Me is Mg, Zn, and Ca), a charge of the following compositions was prepared: $MgSO_4$ (MgO 14.7%, WO_3 85.3%); $ZnSO_4$ (ZnO 26%, WO_3 74%); or $CaWO_4$ (CaO 19.5%, WO_3 80.5%). After stirring for 2 h, the charge was poured into the crucible and pressed to the surface level. The modes of radiation treatment during the synthesis were selected experimentally, and data on the quantitative values of the energy of the electron flux and the power density of the flux are given in the captions and comments to all figures and tables. A typical view of synthesized ceramic samples after exposure to the electron flux with E = 1.4 MeV and a power density in the surface plane of the charge P = 15 kW/cm^2 is shown in Figure 2. During the synthesis, ceramic samples were formed as plates, and the size of the crucible or a series of individual samples took the form of droplets.

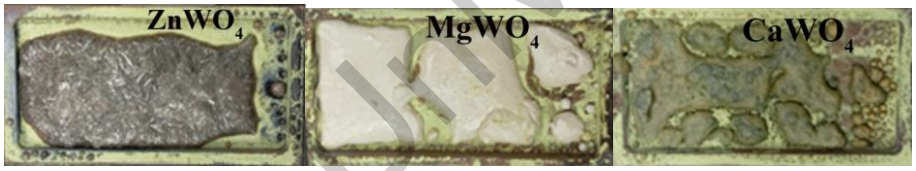

623 **$ZnWO_4$** 624 **$MgWO_4$** 625 **$CaWO_4$**

Figure 2. Photographs of $ZnWO_4$, $MgWO_4$, and $CaWO_4$ ceramic samples synthesized under the influence of an electron flux with E = 1.4 MeV, P = 15 kW/cm^2.

Crucibles with a depth of 10 mm were used for synthesis. A 10 mm thick charge was poured into the crucibles, regardless of the bulk density of the mixture. The bulk density of the charge, depending on the composition, ranged from 1.5 to 2.0 g/cm^3. With such a thickness of the charge layer, in all cases, the electron path depth was less than the layer thickness. Therefore, some of the charge in the lower part of the sample was not converted into ceramics, partially stuck to the bottom of the sample, or remained at the bottom of the crucible.

Part of the charge disappeared from the crucible during the radiation treatment of the charge. The mass loss of the charge was the result of two main processes, including the electrical charging of the particles of dielectric materials with the flow of electrons and an increase in air pressure in the charge when heated.

2.2. Synthesis Efficiency

Basic information about the synthesis results is given in Table 1. The sample numbers in the table correspond to the accounting system adopted by the authors. The synthesis was carried out at an electron energy of E = 1.4 MeV. Samples 510, 512, and 514 and samples 623, 624, and 625 differ in the synthesis time. The second batch was made 3 months after the manufacture of the first. The first batch was synthesized by processing with an electron beam with a power density of P = 18 kW/cm^2, and the second batch was P = 15 kW/cm^2. The same initial powders of metal oxides were used for the synthesis.

Table 1. Efficiency of synthesis of $ZnWO_4$, $MgWO_4$, and $CaWO_4$ ceramic samples.

Sample Number	Charge, Description	Power Density, kW/cm^2	Weight of Samples, g	The Output of the Synthesis Reaction * %	Mass Loss, %	Ceramic Density g/cm^3	Crystal Density g/cm^3
510	$ZnWO_4$ (ZnO 26%, WO_3 74%)	18	86.9	98.7	1.3	5.9	7.79
512	$MgWO_4$ (MgO 14.8%, WO_3 85.2%)	18	71.6	99.3	0.7	3.75	6.89
514	$CaWO_4$ (CaO 19.5%, WO_3 80.5%)	18	50.7	75.7	24.3	3.9	6.06
623	$ZnWO_4$ (ZnO 26%,WO_3 74%)	15	64.6	91.3	8.9	6.38	7.79
624	$MgWO_4$ (MgO 14.8%, WO_3 85.2%)	15	47.3	97.2	2.8	4.26	6.89
625	$CaWO_4$ (CaO 19.5%, WO_3 80.5%)	15	39.5	73.3	26.7	4.1	6.06

* The output of the synthesis reaction: M_0/M_{charge}, where M_0 mass samples in the crucible to the mass of M_{charge} used for the synthesis of the charge.

The samples were removed from the crucible and weighed after completing synthesis. The synthesized samples had a porous structure. The densities of ceramic samples $ZnWO_4$, $MgWO_4$, and $CaWO_4$ (see Table 1) were below the specific density of crystals. It was found that the densities of ceramic samples 623–625 were slightly higher than those of ceramic samples 510, 512, and 514, although the power densities of electron fluxes were lower for them. The efficiency of the radiation synthesis or the yield of the synthesis reaction was estimated as the ratio of the masses of M_0 samples in the crucible to the mass of M_{charge} used for the synthesis of the charge.

An analysis of the results presented in Table 1 demonstrates the satisfactory reproducibility of the radiation synthesis. The efficiency of the ceramic's synthesis from the charge of the same composition with powders of the same background and the same preliminary preparation is similar for those prepared at different times and with different power densities. The values of the synthesis efficiency of $ZnWO_4$ and $MgWO_4$ ceramics are in the range of 91–99%, whereas for $CaWO_4$, this value is in the range of 73–75%. There is a significant difference in the efficiency of the synthesis of ceramics from Zn and Mg oxides on the one hand and for Ca on the other. A comparison of the synthesis efficiencies with the dispersion of the powders used (see Figure 1) allows us to identify the following pattern. If the mixed powders differ in dispersion, then synthesis is realized with high efficiency from a mixture of powders with close dispersion and with low efficiency from different dispersion powders.

It should be noted that the formation of ceramics, indicated by the compositions in Table 1, occurs with high efficiency from the charge composed of the initial metal oxides with significantly different melting temperatures: the melting temperatures of CaO (2572 °C), MgO (2825 °C) are close in value, while the efficiency of the synthesis of ceramics from CaO powders (2572 °C) + WO_3 (1473 °C) is significantly lower in value. As can be seen from the results presented in Figure 1, CaO and WO_3 powders have a large difference in dispersion compared to ZnO + WO_3 and MgO + WO_3 pairs. It is assumed that this phenomenon can be explained by the fact that the role of dispersion of the initial powders is dominant in the synthesis. This takes the dominant role over temperature.

3. Results and Discussions

3.1. The Structure of Ceramic Samples

The surface structure of the synthesized samples of $CaWO_4$, $BaWO_4$, and $CaWO_4$ was studied using a Mira 3 scanning electron microscope (TESCAN). Since the samples under study were dielectrics, the samples were coated with a conductive carbon layer at

the Quorum Q150R ES spraying plant. This study was conducted at an accelerating voltage of 25 kV. SEM images of the measured samples synthesized under the influence of the electron flux with E = 1.4 MeV, P = 18 kW/cm^2 are shown in Figure 3.

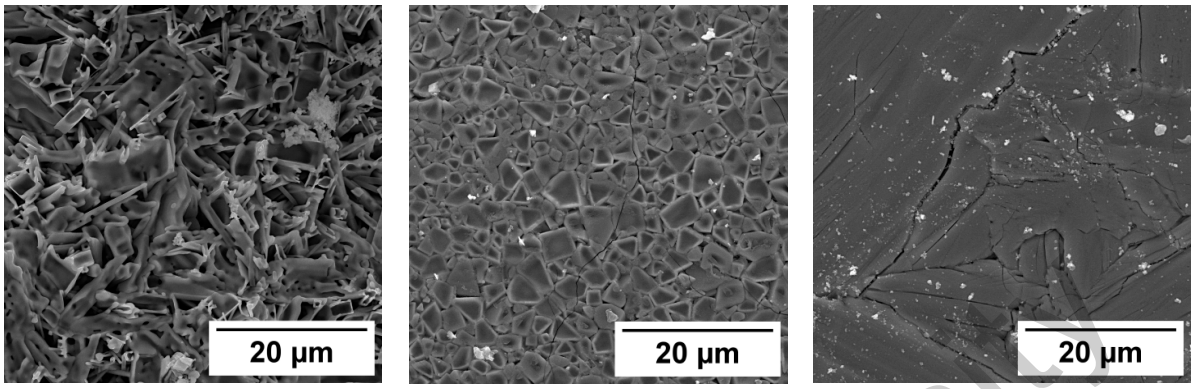

Figure 3. SEM images of the surface of the ceramic samples: (**a**) $ZnWO_4$; (**b**) $MgWO_4$; and (**c**) $CaWO_4$.

A porous microstructure with elongated elements with sizes ranging from 7 to 20 microns and a thickness of about ~7 microns can be observed on the surface of $ZnWO_4$ samples. These elements could be microcrystals of the synthesized substance. Densely packed microcrystals of polyhedral shapes with average sizes ranging from 2 to 5 microns can be observed on the surface of $MgWO_4$ samples. The surface of the $CaWO_4$ sample has the appearance of a solidified melt with cracks. The block sizes range from 5 microns to 100 microns. Cracks, as a rule, are arranged in an orderly manner, parallel to each other. This suggests the possibility of the formation of a crystal structure in the samples.

The presented results suggest the possibility of crystal structure formation in the synthesized samples.

X-ray diffraction patterns were collected using a Bruker D8 ADVANCE diffractometer (AXS, Berlin, Germany) equipped with a scintillation detector in step-scan mode over a diffraction angle range of 10 to 90° 2θ with Cu $K\alpha$ radiation as the source. The experiments were conducted at room temperature, employing a flat sample in Bragg–Brentano geometry (40 kV, 40 mA, 2 s exposure time, and a step size of 0.02° 2θ). Data processing was carried out using the DIFFRACplus software package (version 9.0; Bruker AXS, Billerica, MA, USA), sample identification utilized the Powder Diffraction File (PDF-2) database (ICDD, 2007), and indexing was performed using EVA software (Bruker, 2007). Rietveld profile fitting, the determination of the crystallinity degree, crystallite size, and unit cell parameter refinement were accomplished using the TOPAS 4.2 software package (Bruker, 2008) with the agreement factors (R_{wp}) of Rietveld refinements ranging from 4.0 to 7.9%.

Figure 4 shows the diffraction pattern of the X-ray diffraction pattern of samples 510, 512, and 514 ($ZnWO_4$, $MgWO_4$, and $CaWO_4$), respectively.

The results of the X-ray powder diffraction investigation are presented in Table 2. The qualitative phase analysis and indexing of the diffraction patterns utilized the data from the PDF-2 database (ICDD, 2007). The table also shows the results of a study of the structure of samples obtained during synthesis in the "no scan" mode.

Sample 511 primarily consists of the following phases: magnesium tungsten oxide ($MgWO_4$) (tetragonal, PDF 00-052-0390), tungsten oxide (W_3O_8) (PDF 01-081-2262), and magnesium tungsten oxide ($MgWO_4$) (triclinic, PDF 00-045-0412).

Sample 512 primarily consists of the following phases: magnesium tungsten oxide ($MgWO_4$) (tetragonal, PDF 00-052-0390) and tungsten oxide (WO_3) (PDF 01-072-0677).

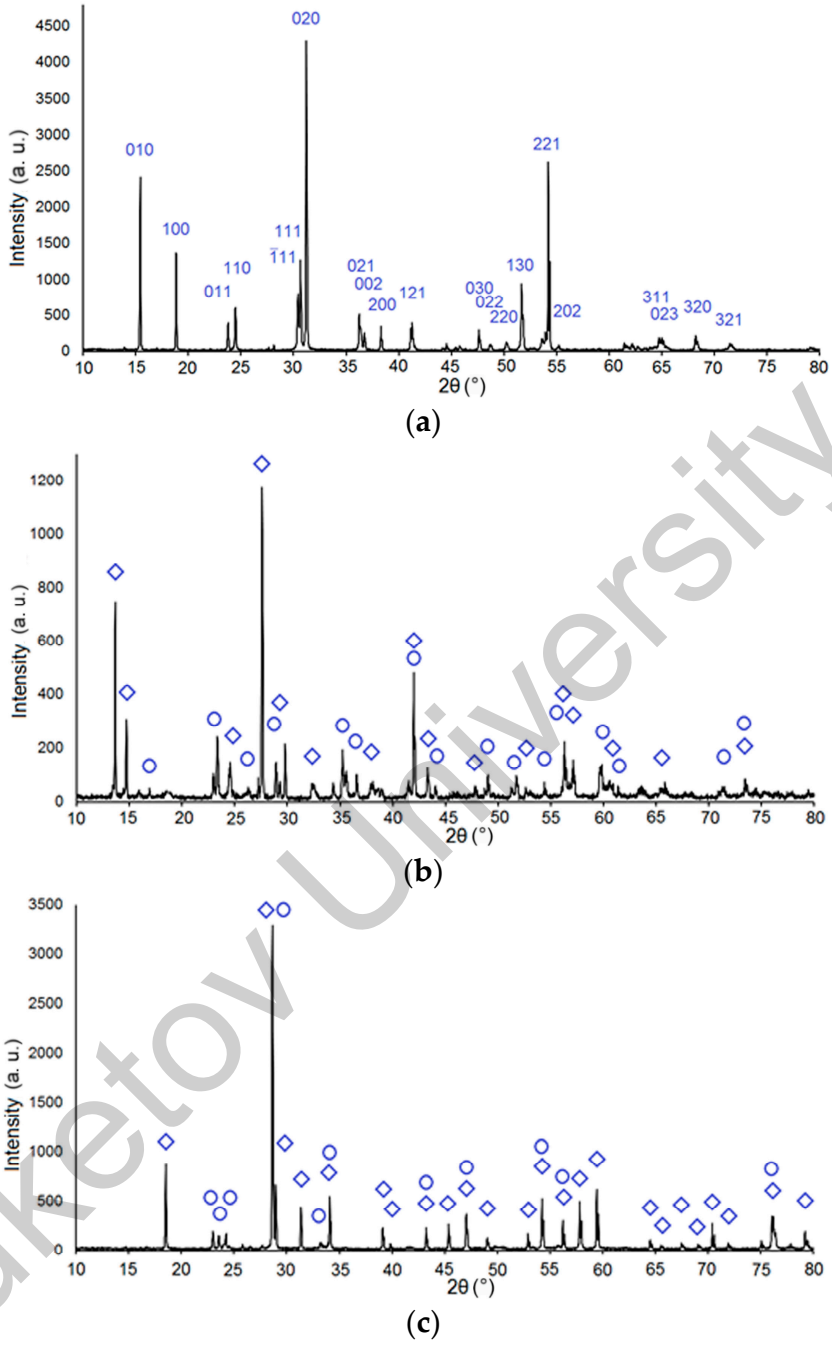

Figure 4. X-ray diffraction pattern of samples (**a**) 510, (**b**) 512, and (**c**) 514. The hkl indices of the reflexes of $ZnWO_4$ are marked. Reflections belonging to $MgWO_4$ (tetragonal), $CaWO_4$, and WO_3 are marked with ◊ and o, respectively.

Following the results presented in Figure 4 and in Table 1, a crystalline phase of the corresponding composition was detected in all synthesized samples, regardless of the synthesis modes. Also, additional phases were found in samples 511–514 in small quantities of tungsten oxide (W_3O_8) and triclinic magnesium tungsten oxide in $MgWO_4$ and WO_3 sample 513 in $CaWO_4$.

Nevertheless, the results of XRD studies show that during the radiation treatment of the charge, ceramics were formed mainly with the crystalline phases $ZnWO_4$, $MgWO_4$, and $CaWO_4$.

Table 2. The results of the phase composition investigation.

Sample Number *	Phase	Degree of Crystallinity	Crystallite Size	Refined Unit Cell Parameters
509	$ZnWO_4$	99.9 (±5) %	131 (±15) nm	P2/c, a = 4.689(4) Å, b = 5.716(7) Å, c = 4.925(3) Å, β = 90.6(1) °, V = 132.0(1) Å^3
510	$ZnWO_4$	99.8 (±5) %	113 (±11) nm	P2/c, a = 4.691(4) Å, b = 5.718(7) Å, c = 4.927(3) Å, β = 90.6(1) °, V = 132.1(1) Å^3
511	See below			
512	See below			
513	$CaWO_4$ (~86%)	99.9 (±5) %	167 (±35) nm	I41/a, a = 5.243(2) Å, c = 11.371(4) Å, V = 312.5(2) Å^3
	WO_3 (~14%)		114 (±28) nm	P21/n, a = 7.311(2) Å, b = 7.532(2) Å, c = 7.694(2) Å, β = 90.8(1) °, V = 423.6(1) Å^3
514	$CaWO_4$ (~92%)	99.7 (±5) %	200 (±32) nm	I41/a, a = 5.242(1) Å, c = 11.372(4) Å, V = 312.5(1) Å^3
	WO_3 (~8%)		127 (±24) nm	P21/n, a = 7.318(4) Å, b = 7.559(3) Å, c = 7.694(4) Å, β = 90.8(1) °, V = 425.6(3) Å^3

* Note: samples with even and odd numbers are similar and have the same composition but were synthesized under different modes, "with scanning" (even) and "without scanning", in order to show the independence of the result from the synthesis modes.

3.2. Cathodoluminescence Spectra

Crystals and ceramics based on tungstates are promising for use as scintillators. The main characteristics of scintillators are the efficiency of converting absorbed radiation energy into light, luminescence spectra, and its attenuation time. The production of ceramics with the characteristics necessary for scintillators, including exposing a radiation stream to a charge from a mixture of metal oxides, is currently at the stage of proving the possibility of such synthesis. We studied the spectral and kinetic characteristics of the cathodoluminescence (CL) and photoluminescence (PL) of synthesized ceramic samples $ZnWO_4$, $MgWO_4$, and $CaWO_4$.

An electron accelerator was used as a source of the excitation of cathodoluminescence, generating single pulses with the following characteristics: electron energy—0.25 MeV; pulse duration at half-height—10 ns; current density at maximum up to 100 A/cm^2; and excitation energy density per pulse, which can vary in the range from 1 to 50 mJ/cm^2.

Luminescence was recorded with a photomultiplier PMT-97 using an MDR-23 monochromator (spectral sensitivity range 200–2000 nm, linear dispersion 1.3 nm/mm) and a Tektronix DPO3034 digital oscilloscope (300 MHz). The integrated spectra of the CL were recorded using the fiber-optic spectrometer AvaSpec-2048 (200–1100 nm). The integral luminescence spectrum can be understood as the spectrum that is measured over the

entire time of illumination after exposure to an excitation pulse. The luminescence spectra were corrected for the spectral sensitivity of the optical path of the measurement system. When electrons excite the used energies, at least 99% of the total absorbed energy of the flow is spent on creating electron-hole excitations in the matrix, and the created electron-hole excitations transfer energy to the centers of luminescence. When exposed to the flow of electrons, excitation occurs at the entire depth of the electron path. The electron ranges for $ZnWO_4$, $MgWO_4$, and $CaWO_4$, whose densities are 7.8, 6.9, and 6.1 g/cm^3, are 0.08–0.11 mm, respectively. Consequently, luminescence, excited by a flow of electrons with an energy of 250 keV, carries information regarding the processes in the volume of matter.

The results of measurements of the integral spectra of the CL and the synthesized ceramic samples are shown in Figure 5. The spectra are presented in a form convenient for comparing their qualitative characteristics (band shapes) but not quantitative ones.

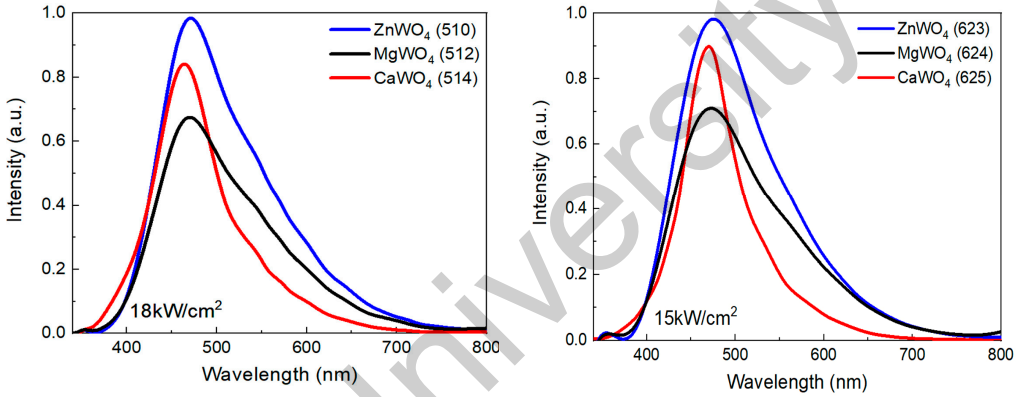

Figure 5. Cathodoluminescence spectra of the samples (**a**) 510, 512, 514 and (**b**) 623, 624, 625.

Figure 5a shows the luminescence spectra of ceramic samples $ZnWO_4$, $MgWO_4$, and $CaWO_4$ synthesized at 18 kW/cm^2 on the left side (samples 510, 512, 514), and the same samples are shown to be synthesized at 15 kW/cm^2 on the right side of Figure 5b (samples 623, 624, 625). The samples differ not only in that they were synthesized using electron fluxes with different power densities but also in the synthesis time. The samples 623, 624, and 625 were synthesized 3 months after the synthesis of the samples 510, 512, and 514. All samples were synthesized from the charge prepared from the same starting materials. The charge was prepared immediately before synthesis. The shape of all luminescence bands was complex. The maxima of the luminescence bands in all the studied samples are clearly pronounced and shifted to the short-wave edge. The long-wavelength edge of the luminescence is distorted by the superposition, clearly of other bands. The characteristics of the bands are summarized in Table 3.

Table 3. Characteristics of cathodoluminescence bands of ceramic samples.

Sample	Sample Number	λ_m, nm	ΔW, eV	Sample Number	λ_m, nm	ΔW, eV
			Cathodoluminescence			
$ZnWO_4$	510	467	0.58	623	472	0.60
$MgWO_4$	512	464	0.57	624	470	0.58
$CaWO_4$	514	468	0.44	625	465	0.44
			Photoluminescence			
$ZnWO_4$	510	482	0.54	623	489	0.54
$MgWO_4$	512	482	0.49	624	480	0.58
$CaWO_4$	514	491	0.48	625	475	0.55

The characteristics of the measured cathodoluminescence spectra of ceramic samples synthesized in the radiation field correspond well to the known photoluminescence spectra of $ZnWO_4$ [26–28], $MgWO_4$ [2,29], and $CaWO_4$ [30] crystals.

The characteristics of the measured cathodoluminescence spectra of $ZnWO_4$ and $MgWO_4$ crystals synthesized in the radiation field of ceramic samples are consistent with the photoluminescence spectra [31].

From the research results presented in Figure 5 and in Table 3, it can be seen that the characteristics of the luminescence bands of the studied ceramics are well reproduced during radiation synthesis from the same starting materials. Luminescence characteristics do not depend on the magnitude of the power density in the range of 15–18 kW/cm^2. The positions of the maxima of the luminescence bands in all types of ceramics are close, ranging from 464 to 572 nm. This may indicate that the structure of luminescence centers is the same for all samples. Oxygen vacancy complexes can be these centers [32]. The possibility of the existence of such complexes is also assumed in other materials based on metal oxides [33,34] and quartz [35]. It should be noted that the cathodoluminescence bands of $ZnWO_4$ and $MgWO_4$ ceramics differ from the band in $CaWO_4$ due to the presence of a structurally complex edge in the long-wavelength region.

3.3. Kinetics of Cathodoluminescence Attenuation

The kinetics of relaxation of luminescence in ceramic samples after excitation by an electron flux pulse with a duration of 10 ns at half-altitude has been studied. The time to resolution of the stand used is 10 ns. As the research results have shown, there is no noticeable change in intensity for the relaxation kinetics in the time range of up to 1 microsecond. Figure 6 shows the results of measurements of relaxation kinetics in the range of up to 100 microseconds in semi-logarithmic coordinates.

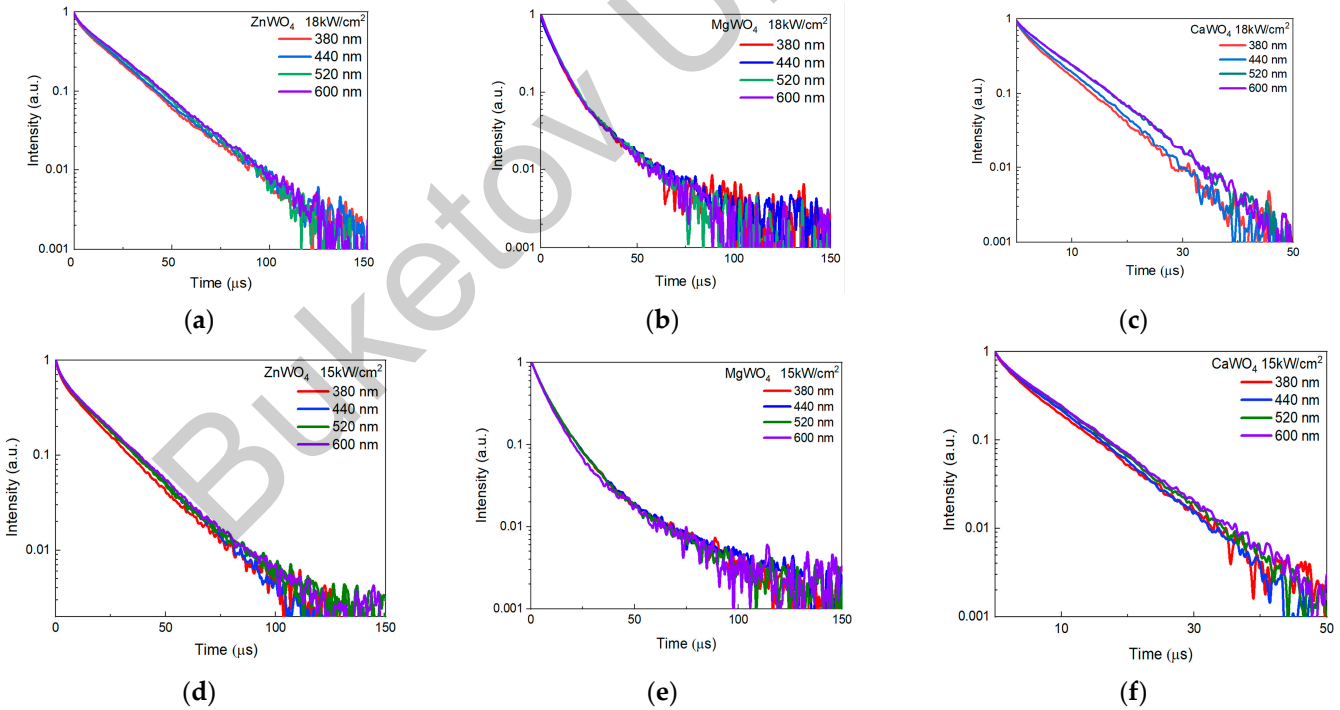

Figure 6. Kinetic curves of luminescence attenuation of ceramic samples at an electron flux power density in the range of 18 kW/cm^2 (**a**) $ZnWO_4$, (**b**) $MgWO_4$, and (**c**) $CaWO_4$ and at an electron flux power density in the range of 15 kW/cm^2 for ceramic samples (**d**) $ZnWO_4$, (**e**) $MgWO_4$, and (**f**) $CaWO_4$.

When the electron flux of $ZnWO_4$ ceramic samples is excited by a pulse, there is a decrease in intensity over the entire time range presented. Two components of the decline

are distinguished with characteristic times τ_1 = 6 μS and τ_2 = 19 μS. In $MgWO_4$, three components of luminescence decay are distinguished with characteristic times τ_1 = 3 μS, τ_2 = 10 μS, and τ_3 = 60 μS. In the kinetics of the decay of the cathodoluminescence of $CaWO_4$ ceramics, τ_1 and τ_2 is equal to 2 and 15 μs. The kinetics of luminescence relaxation are similar to those measured at excitation at 250 nm at 300 K [26,36].

Figure 6a–f shows the kinetic curves of luminescence attenuation for the selected points of the spectra. It can be seen that attenuation occurs with the same characteristics for each type of ceramic across the entire spectrum. Note that the characteristics of the kinetic attenuation curves of samples 510–514 and 623–625 are similar. This demonstrates the reproducibility of the synthesis results and the absence of the influence of changes in the influence of the electron flux power density in the range of 15–18 kW/cm^2.

3.4. Photoluminescence Spectra

The excitation and luminescence spectra of $MgWO_4$, $CaWO_4$, and $ZnWO_4$ ceramic samples were measured, and measurements were made using a CM 2203 Solar spectrofluorimeter. All synthesized samples have a dark color. The excitation energy is absorbed in a thin layer of samples. With this luminescence, a fraction of the excited energy is also absorbed. Therefore, the luminescence intensity is low. The following techniques were used to measure luminescence and excitation spectra. The luminescence bands of ceramics are wide; therefore, measurements of the excitation spectra were performed with the maximum open output slots of the CM 2203 Solar spectrofluorimeter. To measure the luminescence spectra, the samples were excited by radiation from a high-pressure mercury lamp through a UVF 5 light filter in the range of 240–400 nm. The power of such an excitation was sufficient to register luminescence. Luminescence was recorded with the AvaSpec-ULS2048BCL-EVO spectrometer (Avantes, the Netherlands).

The results of measurements of the spectral characteristics of the luminescence are shown in Figure 7.

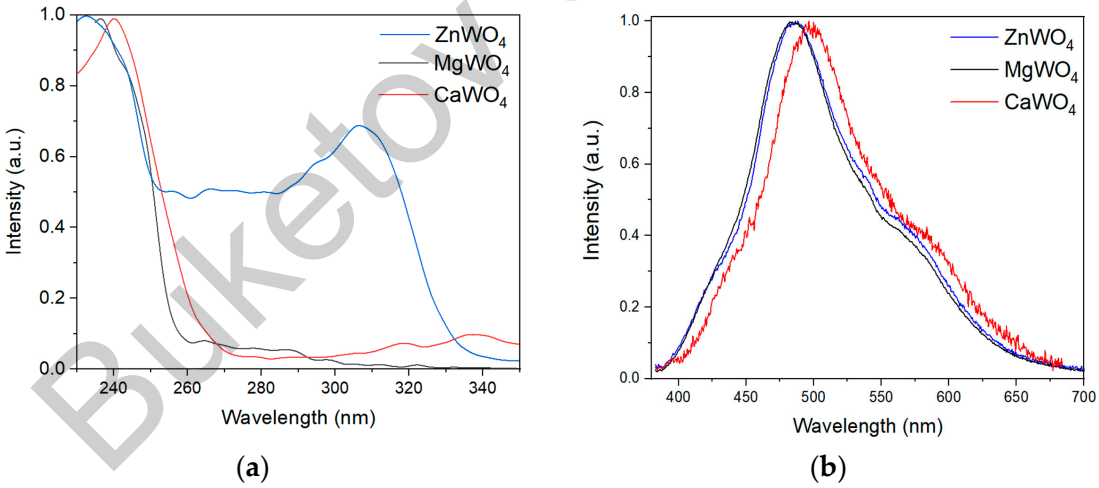

Figure 7. Excitation (**a**,**b**) luminescence spectra of ceramic samples $MgWO_4$, $CaWO_4$, and $ZnWO_4$.

Following from the results presented in Figure 7, luminescence in ceramic samples is excited by radiation at less than 260 nm in $MgWO_4$, 270 nm in $CaWO_4$, and 330 nm in $ZnWO_4$. The photoluminescence spectra are similar to those measured when excited by electrons.

It is assumed that the excitation of luminescence in the range of 250–330 nm for $ZnWO_4$ is due to the existence of nanodefects in highly defective materials [37].

The intensity maxima and values of the photoluminescence bands of the studied samples were determined (see Table 3). A comparison of the results in Table 3 shows that the maxima of the photoluminescence intensities of the samples are shifted to the

long-wavelength region of the spectrum relative to the maxima of the cathodoluminescence spectra of the samples. Perhaps this is due to their absorption in translucent material.

The bandwidth of the photoluminescence spectra is slightly narrower compared to the magnitude ΔW of the cathodoluminescence spectra.

Comparisons of the obtained photoluminescence data of $ZnWO_4$ and $MgWO_4$ samples with the literature data show similar values: λ_m ($ZnWO_4$) = 480 nm [11] for monocrystalline $MgWO_4$ and λ_m = 496 nm (λ_m=2.45 eV; ΔW = 0.7 eV) [38]. Also earlier, in [39], we measured the luminescence spectrum of single-crystal $ZnWO_4$ with a luminescence maximum of λ_m = 490 nm. This result was close to the data in the literature. At the same time, the conditions for recording the luminescence of this reference sample were close to the conditions for recording the photoluminescence of the samples shown in Table 3.

For $CaWO_4$ samples 514 and 625, the measurement results given in this article differ from the results given in the literature data λ_m = 420 nm [11,40] but are close to the results given in [31]. Given that the cathodoluminescence and photoluminescence spectra of $CaWO_4$ samples have similar values of λ_m and ΔW (Table 3), it is necessary to conduct a separate study aimed at studying the properties of these samples. It was also found that the photoluminescence intensity of $CaWO_4$ samples was two orders of magnitude lower than the luminescence intensity of $ZnWO_4$ and $MgWO_4$ at the same optical excitation power.

The presence of detected luminescence during cathode and photoexcitation and compliance with the known spectral properties of luminescence in such crystalline materials indicates the formation of a crystalline phase in synthesized ceramics.

4. Conclusions

This paper presents the results of a new promising method of radiation synthesis of ceramics $ZnWO_4$, $MgWO_4$, and $CaWO_4$. The synthesis was realized from the mixture of powders of Zn, Mg, and Ca oxides with tungsten oxide. The synthesis was carried out by direct action of the powerful electron flux with an energy of 1.4 MeV and flux power density of 15 and 18 kW/cm^2 on the mixture of powders in the crucible. Powders with measured dispersion were used for synthesis. Porous samples with sizes up to 40 × 90 × 5 mm^3, weighing from 40 to 86 g in 10 s, were obtained from the used starting materials. The beam of high-energy electrons acted on each elementary region of the powder in the crucible for 1 s; that is, the synthesis time did not exceed 1 s. This synthesis was carried out without the use of any additional substances to facilitate the process and other additional energy sources.

The structures and luminescent properties of synthesized ceramics $ZnWO_4$, $MgWO_4$, and $CaWO_4$ have been studied. Synthesized ceramics consist mainly of finely dispersed crystals with a crystalline phase. The average crystallite sizes were 110–200 nm. The cathodoluminescence spectra were excited by pulses of the electron flux with a duration of 10 ns, and photoluminescence was similar to those measured for crystals. This confirmed the formation of a crystalline phase during synthesis. Consequently, the resulting $MeWO_4$ ceramics can be used for the same purposes as crystals.

The radiation synthesis of $ZnWO_4$, $MgWO_4$, and $CaWO_4$ ceramics with the properties of crystalline samples was unexpected. The synthesis of $MeWO_4$ was realized under the same radiation treatment conditions as the ceramics of yttrium-aluminum garnet and fluorides of alkaline earth metals from starting materials with lower melting points. Consequently, the totality of the processes of formation of a new phase determined not (or not only) the temperature regime. However, it is clear that the high temperature in the area of the reaction zone promotes synthesis. It is unclear why the radiation synthesis of $MeWO_4$ is effective from a mixture of WO_3 powders (1473 °C) and metal oxides with significantly different melting temperatures: ZnO (1975 °C), CaO (2572 °C), and MgO (2852 °C). Note that the synthesis efficiency of $MgWO_4$ ceramics is higher than $CaWO_4$ ceramics. The efficiency values of the $MgWO_4$ and $CaWO_4$ samples differ, although the melting point of CaO (2572 °C) is lower than that of MgO (2852 °C). A possible explanation for this phenomenon is the assumption discussed in [24] that in dielectric materials, synthesis in

the field of a powerful electron flux is realized with the participation of other physico-chemical processes other than thermal ones. Such processes include ionization. At a high-power density of exposure to harsh radiation, an ion–electron plasma is formed in the charge, which ensures the effective exchange of elements between the particles of the starting substances and the formation of a new phase.

Author Contributions: Conceptualization, V.L. and G.A.; methodology, V.L. and I.C.; software, S.T. and A.T.; validation, V.L. and G.A.; formal analysis, V.L. and Z.B.; investigation, Z.B., V.V., E.K., and I.C.; resources, V.L. and I.C.; data curation, V.L. and Z.B.; writing—original draft preparation, V.L., D.A., and A.T.; visualization, A.T.T. and D.A.; project administration, G.A.; funding acquisition, G.A. All authors have read and agreed to the published version of the manuscript.

Funding: This research was funded by the Science Committee of the Ministry of Science and Higher Education of the Republic of Kazakhstan (Grant No. AP19579177).

Institutional Review Board Statement: Not applicable.

Informed Consent Statement: Not applicable.

Data Availability Statement: The original contributions presented in the study are included in the article, further inquiries can be directed to the corresponding author.

Acknowledgments: Work on the synthesis of ceramics and ICL measurements was carried out by TPU and INP SB RAS under the project of the Russian Science Foundation of the Russian Federation (Grant No. 23-73-00108). In this work, for the analysis of powder dispersibility, we used the equipment of the CCU NMNT TPU, supported by the project of the Ministry of Education and Science of Russia No. 075-15-2021-710.

Conflicts of Interest: The authors declare no conflicts of interest. The funders had no role in the design of the study; in the collection, analyses, or interpretation of the data; in the writing of the manuscript; or in the decision to publish the results.

References

1. Mikhailik, V.B.; Kraus, H. Performance of Scintillation Materials at Cryogenic Temperatures. *Phys. Status Solidi B* **2010**, *247*, 1583–1599. [CrossRef]
2. Dev Bhuyan, P.; Deobrat, S.; Shivam, K.; Sinha, E. Experimental and Theoretical Analysis of Electronic and Optical Properties of $MgWO_4$. *J. Mater. Sci.* **2017**, *52*, 4934–4943. [CrossRef]
3. Mikhailik, V.B.; Kraus, H.; Kapustyanyk, V.; Panasyuk, V.; Prots, Y.; Tsybulskyi, V.; Vasylechko, L. Structure, Luminescence and Scintillation Properties of the $MgWO_4$-$MgMoO_4$ System. *J. Phys. Condens. Matter* **2008**, *20*, 365219. [CrossRef]
4. Chernov, S.; Grigorjeva, L.; Millers, D.; Watterich, A. Luminescence Spectra and Decay Kinetics in $ZnWO_4$ and $CdWO_4$ Crystals. *Phys. Status Solidi B* **2004**, *241*, 1945–1948. [CrossRef]
5. Derraji, K.; Lucena, L.; Favotto, C.; Valmalette, J.-C.; Villain, S.; Nolibe, G.; Lyoussi, A.; Guinneton, F.; Gavarri, J.-R. Structural, vibrational and photoluminescence properties of samarium doped cobalt tungstates. *J. Mol. Struct.* **2022**, *1254*, 131983. [CrossRef]
6. Sofronov, D.S.; Sofronova, E.M.; Starikov, V.V.; Voloshko, A.Y.; Baymer, V.N.; Kudin, K.A.; Matejchenko, P.V.; Mamalis, A.G.; Lavrynenko, S.N. Microwave Synthesis of Cadmium and Zinc Tungstates. *J. Mater. Eng. Perform.* **2012**, *21*, 2323–2327. [CrossRef]
7. Mikhailik, V.B.; Kraus, H.; Miller, G.; Mykhaylyk, M.S.; Wahl, D. Luminescence of $CaWO_4$, $CdMoO_4$, and $ZnWO_4$ scintillating crystals under different excitations. *J. Appl. Phys.* **2005**, *97*, 083523. [CrossRef]
8. Itoh, M.; Fujita, N.; Inabe, Y. X-Ray Photoelectron Spectroscopy and Electronic Structures of Scheelite- and Wolframite-Type Tungstate Crystals. *J. Phys. Soc. Jpn.* **2006**, *75*, 084705. [CrossRef]
9. Nagornyi, V.; Feldbach, E.; Jonsson, L.; Kirm, M.; Kotlov, A.; Lushchik, A.; Nefedov, V.; Zadneprovski, B. Energy transfer in $ZnWO_4$ and $CdWO_4$ scintillators. *Nucl. Instrum. Methods Phys. Res. A* **2002**, *486*, 395–398. [CrossRef]
10. Pereira, P.F.S.; Gouveia, A.F.; Assis, M.; de Oliveira, R.C.; Pinatti, I.M.; Penha, M.; Goncalves, R.F.; Gracia, L.; Andres, J.; Longo, E. $ZnWO_4$ nanocrystals: Synthesis, morphology, photoluminescence and photocatalytic properties. *Phys. Chem. Chem. Phys.* **2018**, *20*, 1923–1937. [CrossRef]
11. Kraus, H.; Mikhailik, V.B.; Ramachers, Y.; Day, D.; Hutton, K.B.; Telfer, J. Feasibility study of a $ZnWO_4$ scintillator for exploiting materials signature in cryogenic WIMP dark matter searches. *Phys. Lett. B* **2005**, *610*, 37–44. [CrossRef]
12. Belli, P.; Bernabei, R.; Borovlev, Y.A.; Cappella, F.; Caracciolo, V.R.; Cerulli, F.A.; Danevich, V.Y.; Degoda, A.; Incicchitti, D.V.; Kasperovych, G.; et al. Optical, luminescence, and Scintillation Properties of Advanced $ZnWO_4$ Crystal Scintillators. Creative Commons Attribution 4.0 International. 2022, pp. 1–14. Available online: https://arxiv.org/ftp/arxiv/papers/2202/2202.10111.pdf (accessed on 18 February 2024).

13. Priyanka, K.P.; Sabu, N.A.; Sunny, A.T.; Sheena, P.A.; Varghese, T. Effect of Electron Beam Irradiation on Optical Properties of Manganese Tungstate Nanoparticles. *J. Nanotechnol.* **2013**, *2013*, 1–6. [CrossRef]
14. Ganiger, S.K.; Chaluvaraju, B.; Ananda, S.R.; Murugendrappa, M. A Feasibility Study of Polypyrrole/Zinc Tungstate (Ceramics) Nano Composites for D. C. Conductivity and as a Humidity Sensor. *Mater. Today Proc.* **2018**, *5*, 2803–2810. [CrossRef]
15. de Macedo, O.B.; de Oliveira, A.L.M.; dos Santos, I.M.G. Zinc tungstate: A review on its application as heterogeneous photocatalyst. *Cerâmica* **2022**, *68*, 294–315. [CrossRef]
16. Fang, J.; Hurley, N.; Chien, C.T.; Guo, A.; Khan, T.A.; Li, M.; Cotlet, M.; Moretti, F.; Bourret, E.; Shifman, S.; et al. Probing the optical properties and toxicological profile of zinc tungstate nanorods. *J. Chem. Phys.* **2024**, *160*, 234701. [CrossRef] [PubMed]
17. Korzhik, M.; Brinkmann, K.-T.; Dormenev, V.; Follin, M.; Houzvicka, J.; Kazlou, D.; Kopal, J.; Mechinsky, V.; Nargelas, S.; Orsich, P.; et al. Ultrafast PWO scintillator for future high energy physics instrumentation. *Nucl. Instrum. Methods Phys. Res.* **2022**, *1034*, 166781. [CrossRef]
18. Belli, P.; Bernabei, R.; Borovlev, Y.; Cappella, F.; Caracciolo, V.; Cerulli, R.; Danevich, F.; Degoda, V.; Incicchitti, A.; Kasperovych, D.; et al. Optical, luminescence, and scintillation properties of advanced $ZnWO_4$ crystal scintillators. *Nucl. Instrum. Methods Phys. Res.* **2022**, *1029*, 166400. [CrossRef]
19. Galashov, E.N.; Gusev, V.A.; Shlegel, V.N.; Vasiliev, Y.V. Growing of $ZnWO_4$ Single Crystals from Melt by the Low Thermal Gradient Czochralski Technique (LTG Cz). *Funct. Mater.* **2009**, *16*, 63–66.
20. Galashov, E.N.; Gusev, V.A.; Shlegel, V.N.; Vasiliev, Y.V. The growth of $ZnWO_4$ and $CdWO_4$ single crystals from melt by the low thermal gradient Czochralski technique. *Cryst. Rep.* **2009**, *54*, 689. [CrossRef]
21. Pourmasoud, S.; Eghbali-Arani, M.; Ameri, V.; Rahimi-Nasrabadi, M.; Ahmadi, F.; Sobhani-Nasab, A. Synthesis of some transition MWO_4 (M: Mn, Fe, Co, Ni, Cu, Zn, Cd) nanostructures by hydrothermal method. *J. Mater. Sci. Mater. Electron.* **2019**, *30*, 8105–8144. [CrossRef]
22. Oliveira, Y.; Costa, M.; Jucá, A.; Silva, L.; Longo, E.; Arul, N.; Cavalcante, L. Structural characterization, morphology, optical and colorimetric properties of $NiWO_4$ crystals synthesized by the co-precipitation and polymeric precursor methods. *J. Mol. Struct.* **2020**, *1221*, 128774. [CrossRef]
23. Lisitsyn, V.; Tulegenova, A.; Golkovski, M.; Polisadova, E.; Lisitsyna, L.; Mussakhanov, D.; Alpyssova, G. Radiation Synthesis of High-Temperature Wide-Bandgap Ceramics. *Micromachines* **2023**, *14*, 2193. [CrossRef] [PubMed]
24. Lisitsyn, V.; Tulegenova, A.; Kaneva, E.; Mussakhanov, D.; Gritsenko, B. Express Synthesis of YAG:Ce Ceramics in the High-Energy Electrons Flow Field. *Materials* **2023**, *16*, 1057. [CrossRef] [PubMed]
25. Lisitsyn, V.; Polisadova, E.; Lisitsyna, L.; Tulegenova, A.; Denisov, I.; Golkovski, M. Efficiency Dependence of Radiation-Assisted Ceramic Synthesis Based on Metal Oxides and Fluorides on Initial Powder Particle Sizes. *Photonics* **2023**, *10*, 1084. [CrossRef]
26. Itoh, M.; Katagiri, T.; Aoki, T.; Fujita, M. Photo-stimulated luminescence and photo-induced infrared absorption in $ZnWO_4$. *Radiat. Meas.* **2007**, *42*, 545–548. [CrossRef]
27. Kolobanov, V.; Kamenskikh, I.; Mikhailin, V.; Shpinkov, I.; Spassky, D.; Zadneprovsky, B.; Potkin, L.; Zimmerer, G. Optical and luminescent properties of anisotropic tungstate crystals. *Nucl. Instrum. Methods Phys. Res. Sect. A Accel. Spectrometers Detect. Assoc. Equip.* **2002**, *486*, 496–503. [CrossRef]
28. Lisitsyn, V.M.; Valiev, D.T.; Tupitsyna, I.A.; Polisadova, E.F.; Oleshko, V.I.; Lisitsyna, L.A.; Andryuschenko, L.A.; Yakubovskaya, A.G.; Vovk, O.M. Effect of particle size and morphology on the properties of luminescence in $ZnWO_4$. *J. Lumin.* **2014**, *153*, 130–135. [CrossRef]
29. Mikhailik, V.B.; Kraus, H. Scintillators for Cryogenic Applications: State-of-Art. *J. Phys. Stud.* **2010**, *14*, 4201. [CrossRef]
30. Yakovyna, V.; Zhydachevskii', Y.; Mikhailik, V.B.; Solskii, I.; Sugak, D.; Vakiv, M. Effect of thermo-chemical treatments on the luminescence and scintillation properties of $CaWO_4$. *Opt. Mater.* **2008**, *30*, 1630–1634. [CrossRef]
31. Lisitsyn, V.; Lisitsyna, L.; Akilbekov, A.; Tupitsyna, I.; Dauletbekova, A.; Zdorovets, M. Photoluminescence of oxygen doped crystals of $ZnWO_4$. In Proceedings of the 12th Europhysical Conference on Defects in Insulating Materials, University of Kent, Canterbury, UK, 13–19 July 2014.
32. Zehani, F.; Sebais, M. UV-visible emission of (O^{2-}–F^{+}) centres in KBr. *Cryst. Res. Technol.* **2007**, *42*, 1123–1125. [CrossRef]
33. Kotomin, E.A.; Popov, A.I. Radiation-induced point defects in simple oxides. *Nucl. Instrum. Methods Phys. Res.* **1998**, *141*, 1–15. [CrossRef]
34. Zvonarev, S.V.; Kortov, V.S.; Shtang, T.V.; Ananchenko, D.V.; Petrovykh, K.A. Effect of structural changes on luminescent and dosimetric properties of nanoscale aluminum oxide. *Appl. Radiat. Isot.* **2015**, *95*, 44–47. [CrossRef]
35. Garmysheva, T.Y.; Shendrik, R.Y.; Paklin, A.S.; Shalaev, A.A.; Kaneva, E.V.; Nepomnyashchikh, A.I. Luminescence of Oxygen-Deficient Centers in Quartz Glasses. *Glass Phys. Chem.* **2022**, *48*, 232–235. [CrossRef]
36. Grassmann, H.; Moser, H.-G. Scintillation properties of $ZnWO_4$. *J. Lumin.* **1985**, *33*, 109–113. [CrossRef]
37. Lisitsyn, V.; Lisitsyna, L.; Tulegenova, A.; Ju, Y.; Polisadova, E.; Lipatov, E.; Vaganov, V. Nanodefects in YAG:Ce-Based Phosphor Microcrystals. *Crystals* **2019**, *9*, 476. [CrossRef]
38. Krutyak, N.R.; Spassky, D.A.; Tupitsyna, I.A.; Dubovik, A.M. Influence of peculiarities of electronic excitation relaxation on luminescent properties of $MgWO_4$. *Opt. Spectrosc.* **2016**, *121*, 45–51. [CrossRef]

39. Alpyssova, G.K.; Afanasyev, D.A.; Bakieva, Z.K.; Lisitsyna, L.A.; Golkovski, M.G.; Tussupbekova, A.K.; Kissabekova, A.A.; Tuleuov, S.D. Optical properties of $ZnWO_4$ ceramics obtained by radiation synthesis. *Bull. Univ. Karaganda-Phys.* **2024**, *3. in press*.
40. Yi, S.-S.; Jung, J.-Y. Calcium Tungstate Doped with Rare Earth Ions Synthesized at Low Temperatures for Photoactive Composite and Anti-Counterfeiting Applications. *Crystals* **2021**, *11*, 1214. [CrossRef]